

Deep Neural Network Based Modelling of Chemisorption Process on Surface of Oxide Based Gas Sensors

Rahul Gupta^{1,2*}, Pradeep Kumar¹ & Dinesh Kumar^{3,4}

¹J. C. Bose University of Science and Technology, YMCA, Faridabad 121 006, Haryana, India

²University Institute of Engineering and Technology, Kurukshetra University, Kurukshetra 136 119, Haryana, India

³Department of Electronic Science, Kurukshetra University, Kurukshetra 136 119, Haryana, India

⁴Gurugram University, Gurugram 122 003, Haryana, India

Received 9 June 2023; revised 30 August 2023; accepted 11 October 2023

The sensor response of the metal oxide based gas sensor has been simulated using Deep Neural Network (DNN) model. The neural network designed for the modelling of the sensor has single input layer, three hidden layers and single output layer. The linear regression algorithm has been used to compute the electrical conductance of the sensor at given temperature and pressure. The data generated through modified Wolkenstein method has been used for training, validation and testing of the developed network. The data for materials Tin (IV) oxide (SnO₂), Tin (II) oxide (SnO) and Copper (I) oxide (Cu₂O) with different E_g values has been utilized. The other input parameters like Temperature, N_D, N_C, N_V, E_F-E_{SS} and E_{CS}-E_F are varied for the specific range to collect a variety of data for calculation of electrical conductance of the sensor. The total data used for training, validation and testing was 1,90,512 data points. The plots for training, validation and testing phase have been plotted. The sensor response computed through the proposed model is validated with the results of already published mathematical model. The sensor response shows steep change when the gas concentration of the target gas reaches above 10⁻⁸ atm. The proposed model can be retrained or transfer learning can be applied for using the same model for other types of materials for gas sensing applications.

Keywords: Chemisorption, Deep neural network, Gas sensor, Numerical modelling

Introduction

Visual and auditory sensors are commercially available for industrial applications, but reliable chemical sensors for olfaction like applications are still limited. The gas sensors are used in numerous industrial applications like pollution monitoring, chemical industries, breath test for detecting alcohol, shelf-life detection of fruits and vegetables, natural gas leakage detection, medical and health monitoring and other complex chemical sensor systems.¹⁻³ Further, from the entrepreneurial aspect these sensors are a crucial component in all these applications, hence need intensive research in today's competitive world. The electronic nose^{4,5} is such an example of an array of gas sensors complemented with a pattern recognition and machine learning based approach of identifying and classifying gases. A conventional electronic nose comprises of an array of sensors followed by the pre-processing circuit, controller and machine learning framework.⁶⁻⁸ Machine learning

based modelling are explored by many researchers in recent times for industrial applications.⁹⁻¹¹ These types of industrial sensors are likely to play a major role in IoT based applications because of their small size, weight and reduced hardware cost. Further these sensors have the capability of identifying inorganic chemical and Volatile Organic Compounds (VOCs).

Metal oxide-based gas sensors with worthier material surface properties and extended sensing capabilities have been developed using Zinc oxide (ZnO), Titanium dioxide (TiO₂), Silicon dioxide (SiO₂), Nickel (II) oxide (NiO₂), Ferric oxide (Fe₂O₃) and Copper (II) oxide (CuO).¹² The sensing mechanism of these sensors is based upon the electrochemical process between the material and the target gases.¹³⁻¹⁶ The adsorption of target gas at the grain boundaries of the sensor causes interchange of charge. The adsorption process includes oxidation and reduction one by one till the equilibrium is achieved. At equilibrium the generation and degeneration of localized electronic states due to presence of oxygen and target gas is same. These generated electronic

*Author for Correspondence
E-mail: rgupta.iit@gmail.com

states act as trap for negative and positive charged particles. This causes a transfer of charge at the surface of semiconductor and the gas molecules present in the environment. The complete process of adsorption and desorption causes a considerable amount of change in electrical properties of the sensor. The change in electrical conductance varies with the nature of gas and its concentration at the surface of sensor. This needs to be calibrated at given pressure and temperature to identify and compute the target gas concentration.

Chemisorption is a process of direct chemical bonding of an atomic species to a solid-state semiconductor surface.^{17,18} Despite the fundamental feature and significance of chemisorption, linking the internal structure of different materials to their chemisorption properties remains a challenging task. Modelling of many physio-chemical systems requires specific scientific knowledge of the complex processes.^{19,20}

In past decade many researchers have been exploring the possibilities of applying mathematical modelling to further study the characteristics of the gas sensors. The efforts have also been put to increase the selectivity of such sensors for various critical applications.¹⁹⁻²¹ Wolkenstein's model is a mathematical model which helps to understand the changes in electrical properties due to chemical process of adsorption and desorption.²⁰

For such complex chemisorption processes, the modelling of these systems becomes tedious. There are many assumptions which need to be incorporated to mathematically model these complex and non-linear processes. These assumptions lead to the knowledge gap and scientifically make it not suitable for real time applications. Secondly, the data required to model and validate these processes is limited. These data driven machine learning models are black box models and does not incorporate scientific knowledge available in the literature.²²⁻²⁵ Further, combining both scientific knowledge and data driven approach results in better modelling of such processes.

The presented approach is the extension of a data driven model computed using a modified Wolkenstein based model. The data collected using the developed mathematical model is fed to the DNN designed specifically for computation and prediction of electrical conductance of the sensor. Once the neural network is well trained using the developed dataset for SnO₂, SnO and Cu₂O, the network can be

deployed for various other sensor and target gases in real world applications. This will solve various non-linearity involved in the mathematical modelling of semiconductor-based gas sensors.

The emphasis of presented study is on the neural network approach to model the complex non-linear chemisorption process. The theoretical model of chemisorption is discussed in next section of the paper, which has been used as the base for generation of dataset. The basic concept of DNN and the proposed architecture with detailed parameters are given in the manuscript. The simulations results have been explored and discussed along with the conclusion of paper with further future scope of the presented study.

Mathematical Model

The mathematical model computes the Sensor Response (SR) of gas sensor depending upon the process of adsorption at the surface boundaries. The oxygen molecules present in the local surface of sensor dissociates and gets adsorbed within the sensor. After adsorption of oxygen molecules, the process of charge transfer with the surface gets initiated as shown in Fig. 1.

This charge transfer causes the changes in space charge region and results in change in electrical

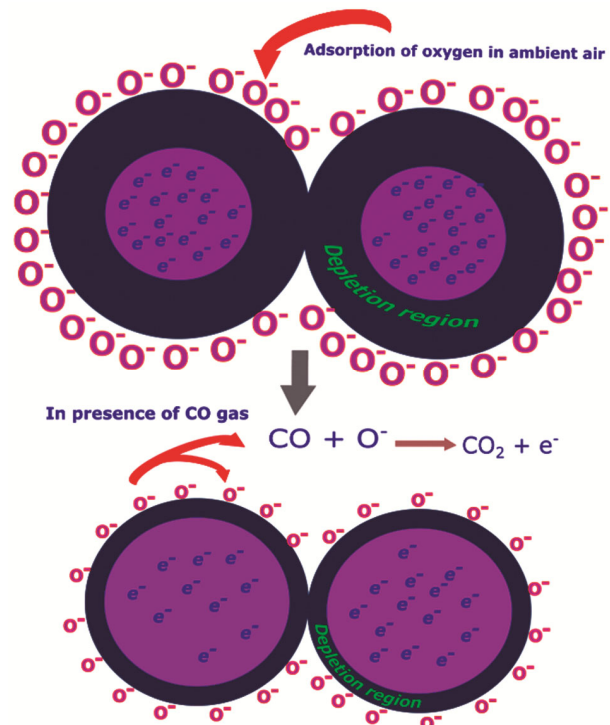


Fig. 1 — Adsorption-desorption process²⁰

properties majorly electrical conductance of the sensor. In similar manner when sensor surface is exposed to target gas like CO the process of desorption takes place. This process further changes the electrical conductance in reverse direction.

The mathematical models developed by researchers tries to model the process of adsorption-desorption and computes the equilibrium point. This equilibrium point then further utilized to compute the Probability Density Spectrum (PDS) of conductance at sensor surface. Further, SR is computed using Eq. (1):

$$Sensor\ Response, SR = \frac{S_{\delta G}(f)\ in\ presence\ of\ CO}{S_{\delta G}(f)\ in\ presence\ of\ O_2} \dots (1)$$

where, $S_{\delta G}(f)$ is the PDS of electrical conductance fluctuation as function of frequency f .

$S_{\delta G}(f)$ mathematical formulation is as shown in Eq. (2):

$$S_{\delta G}(f) = (e\mu_n \frac{s}{Ld})^2 S_{\delta ns}(f) \dots (2)$$

where,

e is the charge of $e^- = 1.6 \times 10^{-19}$ coulombs,

μ_n = Electron mobility,

s = Cross sectional area of sensing layer

L = Length of sensing layer

d is the thickness of the sensing layer typically

The computed sensor response of the sensor at given gas concentration, pressure and temperature is then utilized for further analysis of the sensor properties. This method of mathematical modelling is completely based upon the physical process involved during adsorption-desorption.

Deep Neural Network

An Artificial Neural Network attempts to replicate the structure of neurons inside human brain which can understand the non-linear physical processes. The artificial neural network is formulated by constructing neurons and making there inter connections in a manner that they behave like interconnected brain cells. Neural networks consisting of a large number of neurons (nodes), which are arranged in layers, are called Deep Neural Networks (DNNs). The DNNs have revolutionized artificial intelligence for understanding and solving a variety of complex real-world problems. The DNNs are a type of network that contains a single input layer, multiple hidden layers which allow them to learn nonlinear patterns from input data and finally an output layer. Each and every layer of the network consists of multiple neurons and

every neuron takes multiple inputs and processes it as per the activation function and sends the computed output to the final layer as shown in Fig. 2. The $x_1, x_2, \dots, x_i, \dots, x_n$ are called input nodes and $y_1, y_2, \dots, y_i, \dots, y_m$ are called output nodes of the network. The output nodes for a logistic regression problem are one, for binary classification its value is two and for other complex problems it is on the higher side.

A typical DNN that contains multiple hidden layers, allowing them to learn complex features and nonlinear patterns from input data is shown in Fig. 3. Each layer of a DNN processes the computed value of the previous layer with the help of neurons (nodes), with the final layer producing the resultant of the network. The layers in a DNN are connected by a set of weights ($w_1, w_2, \dots, w_i, \dots, w_l$), which are learned during the training process. Bias is the input independent weight which also needs to be computed and updated during training of the network.

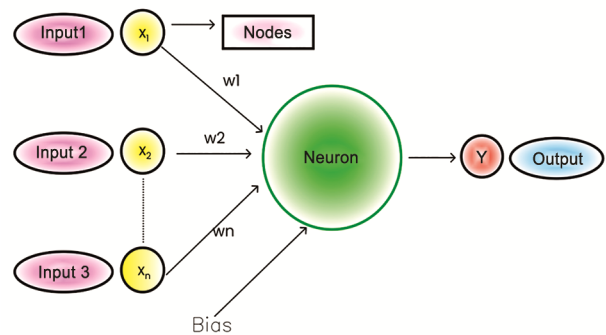


Fig. 2 — Basic structure of neural network

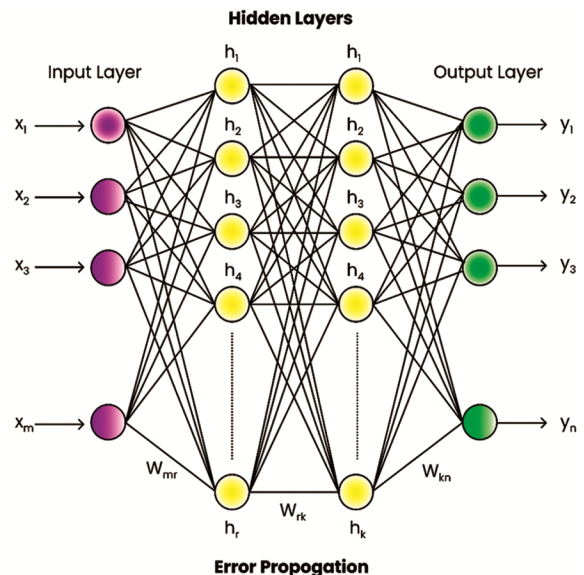


Fig. 3 — Deep neural network architecture

These weights are responsible for further calculation and decision making of a neural network during deployment. The well-trained network with available dataset performs well in unknown situations (real world) as compared to the over or under trained network. The more layers a DNN has, the more complex features it can learn from the input data. However, training a DNN with many layers can be challenging, as the numbers of training parameters like weights, learning rate and gradients parameters varies from small to large range. Thus, an optimal number of nodes and hidden layers are designed for the given data set.

Each node has its own transfer function to compute the output. This activation function takes input x_i and bias b_i along with the weights of edges between node and previous layer nodes as shown in Eq. (3). Activation functions add the non-linearity to the system which is required for modelling a complex system. The output y_i is resultant of computation and denotes the feature extraction of all previous layers and the given node. Each node thus represents a particular pattern in the training data and leads to addition of its own contribution towards the nonlinearity of the system.

$$y_i = \text{Activation_Function}(\sum(w_i * x_i + b_i)) \dots (3)$$

The initial step of implementation of DNN involves adjusting the weights of network to minimize a loss function which is called training of network. The loss function measures the closeness of data towards the desired output, and the target is to find the weights that minimize this function. The most common method for training DNNs is back propagation, in which the gradients of the loss function with respect to the weights are computed and used to update the weights using gradient descent. Other methods, such as stochastic gradient descent and adaptive learning rate methods, are also commonly used. This step is performed using the test dataset typically 70% to 80% of the total dataset. The second step is validation of the computed weights using the validation dataset typically 10% to 15%. Validation step involves application of validation dataset to the trained network and computing the accuracy or other parameters based upon the loss function. Once the desired accuracy is achieved on the validation dataset the training and validation step is over otherwise the network is modified based on analysis of results and both the steps are repeated over again and again. Finally, the deployment and testing

step involving test data or real data is used for real life implementation.

Proposed Work

The non-linearity in the modelling of complex adsorption-desorption processes has been modelled using a DNN. The mathematical models used by various researchers are non-linear in nature and are very complex. Artificial neural networks are one of the possible solutions to derive these models from a data centric approach. The data collected from the mathematical model developed earlier has been used to feed the training of neural networks. The output parameter computed using a neural network is electrical conductance. The data was generated using modified Wolkenstein model equations for the materials SnO₂, SnO and Cu₂O with different E_g values. The other input parameters like Temperature, N_D , N_C , N_V , $E_F - E_{SS}$ and $E_{CS} - E_F$ are varied for the specific range to collect a variety of data for calculation of electrical conductance of the sensor with respect to different materials and gas exposures. The pairwise relationship of various input and output parameters is plotted as show in Fig. 4 using an open-source library seaborn. A two-dimension graph of each data variable is represented to understand the correlation between each data point. Further, the diagonal graphs represent univariate distribution of the data variable, which further helps in deciding the various parameters for DNN. This analysis of data determines the number of nodes and hidden layers in the further developed DNN. The collected data is segmented into three parts for training, validation and testing of neural network.

The neural network architecture with the number of nodes designed to train and predicts the SR is shown in Fig. 5. The designed network has a single input layer, three hidden layers, and one output layer. The input layer has six nodes, three hidden layers have 16, 8 and 4 nodes respectively. The output layer has a single node to represent the electrical conductance of the sensor. This architecture was proposed after various experiments and the rectified linear activation function (ReLU) is used as activation function for each neuron at each stage. The ReLU activation function contributes to the desired non linearity to the system. The output layer activation function is linear as the output of the network is a linear regression problem and the computed value of electrical conductance is floating point value. The Mean Square Error (MSE) has been used to optimize the neural

network for the given dataset. Further the batch size of 32 is used to train the network for 500 epochs. The total data used for training, validation and testing was 1,90,512 which was generated using the modified Wolkenstein model. The experiments have been performed using different combination of layers and nodes. The models were trained and evaluated for accuracy and looked for Overfitting/Underfitting of the model. If the model found to be overfit the number of nodes and layers has been increased and

vice-versa. The presented model with three hidden layers with 16, 8 and 4 nodes has been optimized for the current dataset.

The number of weights (parameters) needed to be computed are shown in Table 1. The number of weights is computed as multiplication of the number of nodes in the $n-1$ layer and the number of nodes in the n layer, in addition to the bias for each node in the present layer.

Total number of parameters (weights) between layer _{i} and layer _{j} = $n_i \times n_j + n_j$

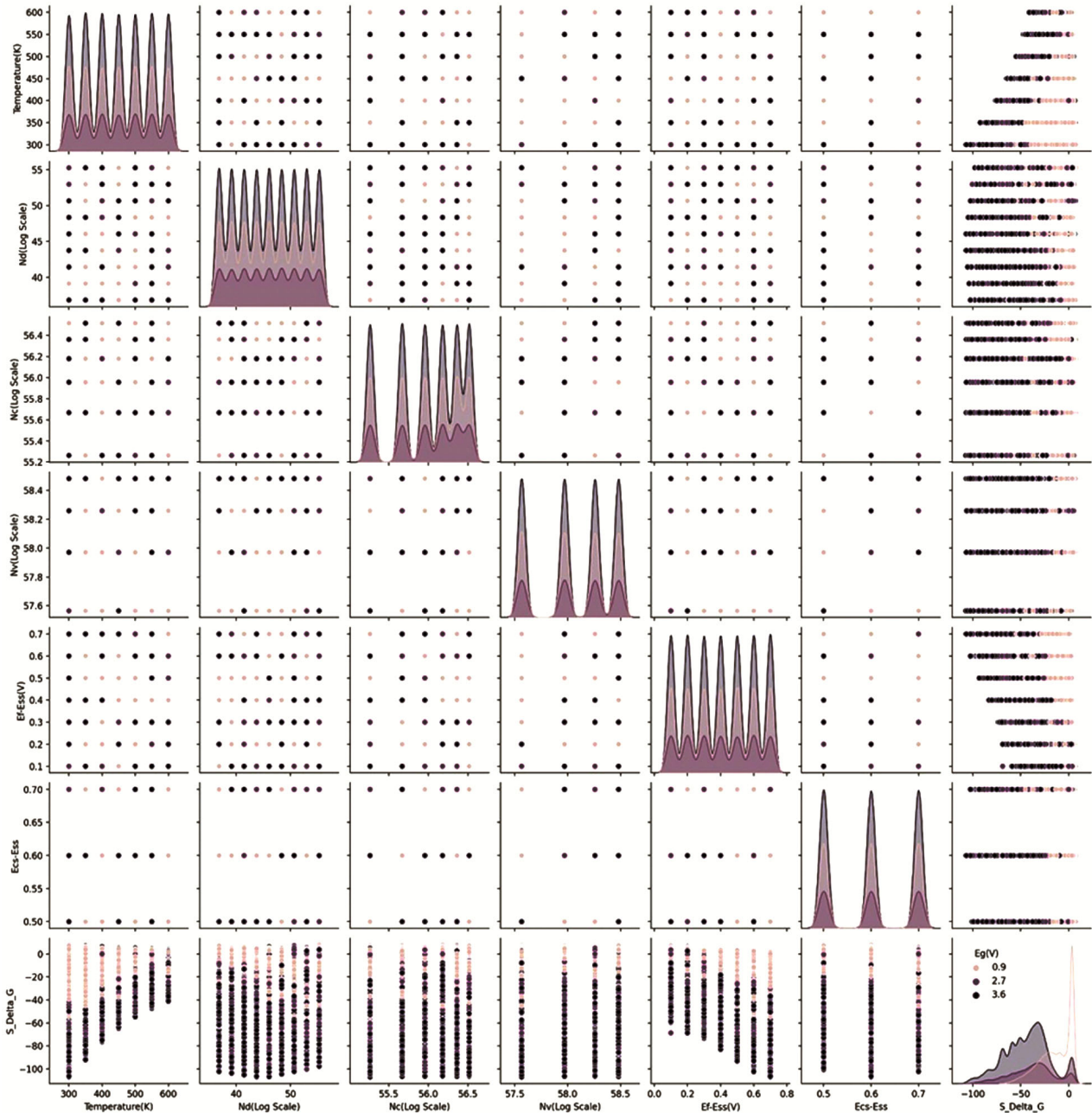


Fig. 4 — Pair wise relationship of data points

where, n_i and n_j are the number of nodes in layer i and j respectively.

So the total number of parameters (weights) for the designed network is $112 + 136 + 36 + 5 = 289$.

Simulation Results and Discussions

The simulation of the presented model has been conducted on Python using jupyter notebook platform. The physical parameters shown in Table 2 which are input for computation of sensor response using Wolkenstein model are used for proposed model. The parameter $E_F - E_{SS}$ represents the difference between Fermi state and induced surface state and it ranges between 0.1 to 0.7eV for different gases and sensor materials. Similarly, the $E_{CS} - E_F$ is the difference between conduction band at surface and

Fermi state. The doping concentration N_D has been fixed in the range of 10^{16} to 10^{24} m^{-2} . The Band Gap E_g has been considered 3.6, 0.9 and 2.7 for materials SnO_2 , SnO and Cu_2O respectively.²⁶ The temperature range considered for the model is 300 to 600K. These parameters are varied over the prescribed range and data has been generated using conventional Wolkenstein model²⁰ and modified Wolkenstein model.²¹ The generated dataset has been used to train, validate and test the presented neural network architecture.

The validation loss during the training of the network is shown in Fig. 6. Initially the validation loss which is the mean square error of the actual and predicted value of electrical conductance was very high during the forward propagation. After a few epochs of training this loss reduces significantly, this occurs due to updating of weights of the network during backward propagation. Once the validation loss stops decreasing the training is halted and the

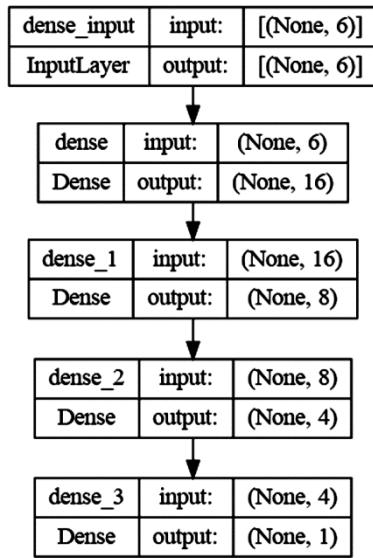


Fig. 5 — Proposed DNN architecture

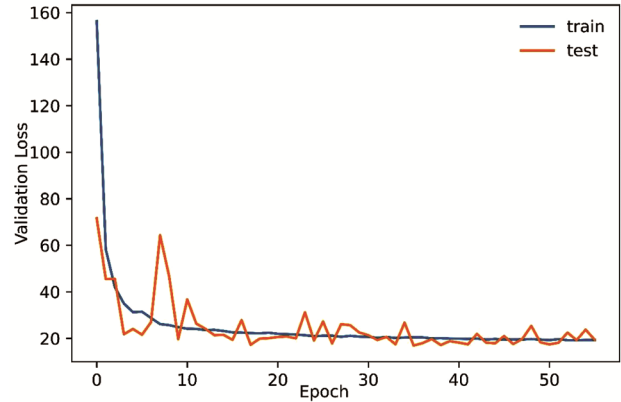


Fig. 6 — Validation loss for training and testing phase with respect to number of epochs

Table 1 — Number of parameters to be computed during training phase

Layer (type)	Output Shape	Computation	Param (weights) #
dense (Dense)	(None, 16)	$6 \times 16 + 6$ (bias)	112
dense_1 (Dense)	(None, 8)	$16 \times 8 + 8$ (bias)	136
dense_2 (Dense)	(None, 4)	$8 \times 4 + 4$ (bias)	36
dense_3 (Dense)	(None, 1)	$4 \times 1 + 1$ (bias)	5

Table 2 — Physical parameters range used for data simulation

Parameter	Symbol	Range
Difference between Fermi level and induced surface states	$E_F - E_{ss}$	0.1 to 0.7 eV
Difference between conduction band at surface and Fermi state	$E_{CS} - E_F$	0.5 to 0.7 eV
Number of available states at Valence band	N_V	10^{25} to $2.5 \times 10^{25} \text{ m}^{-2}$
Doping Concentration	N_D	10^{16} to 10^{24} m^{-2}
Number of available states at Conduction band	N_C	10^{24} to $3.5 \times 10^{24} \text{ m}^{-2}$
Band Gap	E_g	3.6, 0.9 and 2.7
Temperature	T	300 to 650K

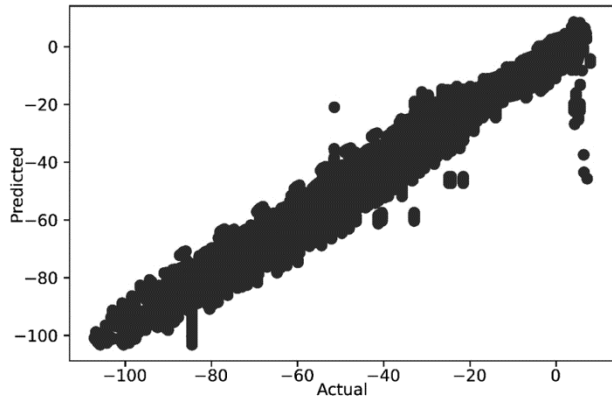


Fig. 7 — Predicted vs Actual plot for training dataset

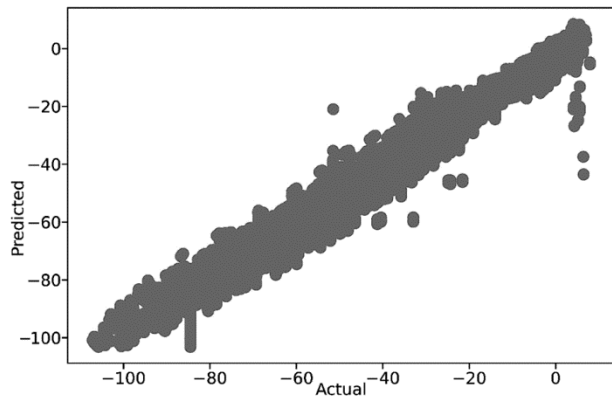


Fig. 8 — Predicted vs Actual plot for Validation dataset

network is set for feeding of validation data. The graph shows that validation data also depicts the same behaviour as depicted by the training data. Once the network weights are updated and the network shows no further improvement in validation loss the training step is completed and the network is available for real life prediction of unknown data i.e. test data.

The prediction of the value of the electrical conductance by the network on the training set is well connected as shown in Fig. 7. There are very few data points which are away from the straight line of Predicted vs Actual value graph. This shows that the network is well trained and it has neither been under fit nor over fit during the training and validation phase. The factor of overfitting is further validated by the Fig. 8 which is on the validation data which has never been shown to the network during the training. The graph of training and validation data is quite similar in nature and hence proves the correct training of the network along with the architecture of the network is therefore perfect fit for the given dataset and problem statement.

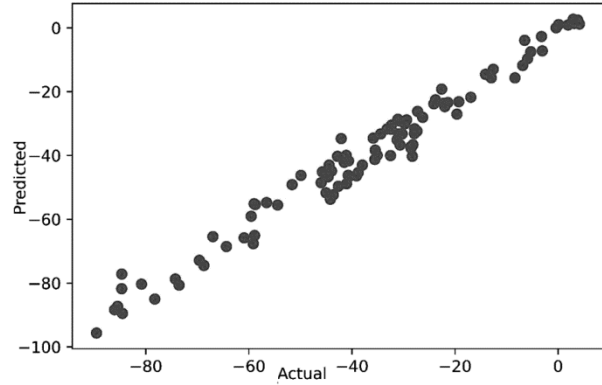


Fig. 9 — Predicted vs Actual plot for test dataset

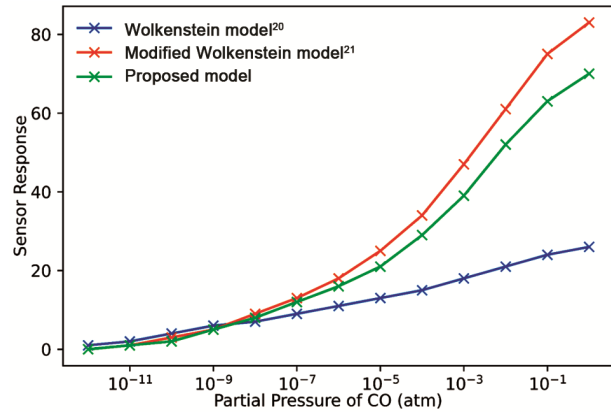


Fig. 10 — Sensor Response comparison of proposed architecture with Wolkenstein model²⁰ and modified Wolkenstein model²¹

Finally, the trained neural network was tested using a test data set which has never been fed to the network during training and validation phase. The results shown in the Fig. 9 shows the straight line for Predicted vs Actual values of the electrical conductance. The straight line in test dataset similar to validation dataset prediction signifies that the training phase (including training and validation step) is neither over fitted nor under fitted. The proposed trained model is ready for deployment phase. This situation is like the real-life environment: if the input values are fed to the network, then it can compute the value of electrical conductance based on the computation of weights of the network.

The plot of the proposed model is shown in Fig. 10 for SR along with the results using the conventional mathematical model and modified Wolkenstein’s approach of oxygen chemisorption. The plot has been generated by applying the desired inputs to the neural network and computing the electrical conductance. Further this computed conductance has been used to compute sensor response from the Eq. (1). The SR

behaviour for the presented neural network is better than both the approaches for the given CO gas concentration. The proposed approach represents the improved sensor response compared to both conventional and modified Wolkenstein's approach. The improved response is due to the fact that the proposed model inherits the non-linear behaviour of chemisorption process. The adsorption-desorption process is a complex process and the neural network approach captures the same during the training phase. The SR for partial pressure under 10^{-9} atm, of compared methods is not distinguishable. When the gas concentration of the target gas reaches above 10^{-8} atm, the SR of the proposed neural based model raises steeply. The discussed behaviour proves that the designed neural network training and validation are done in an optimal manner. The under fitting and over fitting of the network has been taken care of and the network responds to the real-world data in an appropriate manner.

Conclusions

The neural network architecture proposed in this paper for modelling the chemisorption process of adsorption-desorption is well suited for SnO₂, SnO and Cu₂O. The trained model can be used to calculate the electrical conductance of various other semiconductor sensors. The presented model is compared with other mathematical models and found to be performing better for given target gas. The input parameters like Temperature, Band Gap, Doping concentration, Fermi Level etc. will depict the sensor response. The advantage of the presented approach is that it can be applied for other similar materials without going deep into the mathematical derivations and solving complex nonlinear equations. Further, proposed model can be retrained or transfer learning can be applied for using the same model for other types of oxides for gas sensing applications. In future proposed model can be upgraded or modified to cater to larger sets of sensors like array of gas sensors, e-nose applications and other complex industrial applications.

References

- Shankar P & Rayappan J B B, Gas sensing mechanism of metal oxides: The role of ambient atmosphere, type of semiconductor and gases - A review, *Sci Lett*, **126(4)** (2015).
- Barsan N, Koziej D & Weimar U, Metal oxide-based gas sensor research: How to?, *Sens Actuators B: Chem*, **121(1)** (2007) 18–35, <https://doi.org/10.1016/j.snb.2006.09.047>.
- Korotcenkov G, Metal oxides for solid-state gas sensors: What determines our choice?, *Mater Sci Eng B*, **139(1)** (2007) 1–23, <https://doi.org/10.1016/j.mseb.2007.01.044>.
- Li Z, Yu J, Dong D, Yao G, Wei G, He A, Wu H, Zhu H, Huang Z & Tang Z, E-nose based on a high-integrated and low-power metal oxide gas sensor array, *Sens Actuators B: Chem*, **380(1)** (2023) 133289, <https://doi.org/10.1016/J.SNB.2023.133289>.
- Nurputra D, Kusumaatmaja A, Hakim M, Hidayat S, Julian T, Sumanto B, Mahendradhata Y, Saktiawati A, Wasisto H & Triyana K, Fast and noninvasive electronic nose for sning out COVID-19 based on exhaled breath-print recognition, *NPJ Digit Med*, **5(1)** (2021) 115, <https://doi.org/10.21203/rs.3.rs-750988/v1>.
- Sharma N & Liu Y A, A hybrid science-guided machine learning approach for modeling chemical processes: A review, *AIChE J*, **68(5)** (2022) 17609, <https://doi.org/10.1002/aic.17609>.
- Aliyana A K, Kumar S K N, Marimuthu P, Baburaj A, Adetunji M, Frederick T, Sekhar P & Fernandez R E, Machine learning-assisted ammonium detection using zinc oxide/multi-walled carbon nanotube composite based impedance sensors, *Sci Rep*, **11(1)** (2021) 24321, <https://doi.org/10.1038/s41598-021-03674-1>.
- Oh J, Kim S H, Lee M-J, Hwang H, Ku W, Lim J, Hwang I-S, Lee J-H & Hwang J-H, Machine learning-based discrimination of indoor pollutants using an oxide gas sensor array: High endurance against ambient humidity and temperature, *Sens Actuators B: Chem*, **364(1)** (2022) 131894, <https://doi.org/10.1016/J.SNB.2022.131894>.
- Zhang Y & Xu X, Predictions of adsorption energies of methane-related species on Cu-based alloys through machine learning, *Mach Learn*, **3(1)** (2021) 100010, <https://doi.org/10.1016/j.mlwa.2020.100010>.
- Esterhuizen J A, Goldsmith B R & Linic S, Theory-guided machine learning finds geometric structure-property relationships for chemisorption on subsurface alloys, *Chem*, **6(11)** (2020) 3100–3117, <https://doi.org/10.1016/j.chempr.2020.09.001>.
- Toyao T, Suzuki K, Kikuchi S, Takakusagi S, Shimizu K & Takigawa I, Toward effective utilization of methane: Machine learning prediction of adsorption energies on metal alloys, *J Phys Chem C*, **122(15)** (2018) 8315–8326, <https://doi.org/10.1021/acs.jpcc.7b12670>.
- Xiao J, Fu Z, Wang G, Ye X & Xu G, Atomically thin 2D TiO₂ nanosheets with ligand modified surface for ultra-sensitive humidity sensor, *Jiegou Huaxue*, **41(4)** (2022) 2204054–2204060, <https://doi.org/10.14102/j.cnki.0254-5861.2022-0046>.
- Gomri S, Seguin J-L, Guerin J & Aguir K, Adsorption-desorption noise in gas sensors: Modelling using Langmuir and Wolkenstein models for adsorption, *Sens Actuators B: Chem*, **114(1)** (2006) 451–459, <https://doi.org/10.1016/j.snb.2005.05.033>.
- Bejaoui A, Guerin J & Aguir K, Modeling of a p-type resistive gas sensor in the presence of a reducing gas, *Sens Actuators B: Chem*, **181(1)** (2013) 340–347, <https://doi.org/10.1016/j.snb.2013.01.018S>.
- Brinzari V, Korotcenkov G & Boris Y, Chemisorptional approach to kinetic analysis of SnO₂: Pd-based thin

- film gas sensors, *J Optoelectron Adv Mater*, **4(1)**, 2002 147–150.
- 16 Bârsan N, Hübner M & Weimar U, Conduction mechanisms in SnO₂ based polycrystalline thick film gas sensors exposed to CO and H₂ in different oxygen backgrounds, *Sens Actuators B: Chem*, **157(2)** (2011) 510–517, <https://doi.org/10.1016/j.snb.2011.05.011>.
- 17 Gomri S, Seguin J-L & Aguir K, Modeling on oxygen chemisorption-induced noise in metallic oxide gas sensors, *Sens Actuators B: Chem*, **107(2)** (2005) 722–729, <https://doi.org/10.1016/j.snb.2004.12.003>.
- 18 Wolkenstein T, The electron theory of catalysis on semiconductors, *Adv Catal*, **12(1)** (1960) 189–264. [https://doi.org/10.1016/S0360-0564\(08\)60603-3](https://doi.org/10.1016/S0360-0564(08)60603-3).
- 19 Bârsan N, Transduction in semiconducting metal oxide based gas sensors - Implications of the conduction mechanism, *Procedia Eng*, **25(1)** (2011) 100–103, <https://doi.org/10.1016/j.proeng.2011.12.025>.
- 20 Gupta R, Kumar A, Rohilla V, Kumar P, Kumar M & Kumar D, Noise spectroscopy based numerical modelling of chemisorption on SnO₂ surface for CO gas sensing applications, *Micro Nanostructures*, **171(1)** (2022) 207423, <https://doi.org/10.1016/j.micrna.2022.207423>.
- 21 Kumar A, Kumar M, Kumar R, Singh R, Prasad B & Kumar D, Numerical model for the chemical adsorption of oxygen and reducing gas molecules in presence of humidity on the surface of semiconductor metal oxide for gas sensors applications, *Mater Sci Semicond*, **90(1)** (2019) 236–244, <https://doi.org/10.1016/j.mssp.2018.10.020>.
- 22 Pareek V & Chaudhury S, Deep learning-based gas identification and quantification with auto-tuning of hyperparameters, *Soft Comput*, **25(22)** (2021) 14155–14170, <https://doi.org/10.1007/s00500-021-06222-1>.
- 23 Kwon Y M, Oh B, Purbia R, Chae H Y, Han G H, Kim S-W, Choi K-J, Lee Y, Kim J J & Baik J M, High-performance and self-calibrating multi-gas sensor interface to trace multiple gas species with sub-ppm level, *Sens Actuators B: Chem*, **375(1)** (2023) 132939, <https://doi.org/10.1016/J.SNB.2022.132939>.
- 24 Zhai S, Han M, Li Z, Yang S, Duan S & Yan J, M2FL-CCC: Multibranch multilayer feature leaning and comprehensive classification criterion for gas sensor drift compensation, *IEEE Trans Instrum*, **72(1)** (2023) 1–12, <https://doi.org/10.1109/TIM.2023.3296820>.
- 25 Juffry Z H M, Kamarudin K, Adom A H, Miskon M F, Kamarudin L M, Zakaria A, Zakaria S M M S & Abdullah A N, Application of deep neural network for gas source localization in an indoor environment, *Int J Comput Commun*, **18(3)** (2023) 5084, <https://doi.org/10.15837/ijccc.2023.3.5084>.
- 26 Rajshekar K & Kannadassan D, A comprehensive density-of-states model for oxide semiconductor thin film transistors, *J Comput Electron*, **20(6)** (2021) 2331–2341, <https://doi.org/10.1007/s10825-021-01783-8>.